Donor-acceptor graphene-based hybrid materials for managing photoinduced electron-transfer reactions

Anastasios Stergiou, Georgia Pagona and Nikos Tagmatarchis*

Theoretical and Physical Chemistry Institute, National Hellenic Research Foundation, 48 Vassileos Constantinou Avenue, 11635 Athens, Greece.

Email: tagmatar@eie.gr
(*) Corresponding author

Abstract

Graphene research and in particular the topic of chemical functionalization has been exploded in the last decade. The main aim is to induce solubility and thereby enhance processability of the material, which is otherwise insoluble and inapplicable for technological applications when stacked in the form of graphite. In this frame, initially, graphite was oxidized under harsh conditions to yield exfoliated graphene oxide sheets, soluble in aqueous media and amenable to chemical modifications due to the presence of carboxylic acid groups at the edges of the lattice. Some donor-acceptor hybrid materials with photo- and/or electro-active components were prepared and characterized, while their charge-transfer properties were evaluated. However, it was obvious that the highly defected framework of graphene oxide cannot be really utilized in applications that are governed by charge-transfer processes, for example in solar cells. The alternative route for solubilizing and modifying graphene by exfoliating graphite is the current method of choice for the realization of novel hybrid materials and further boost their direct applicability in artificial photosynthesis and the construction of photovoltaic devices. In this review article, the routes for obtaining donor-acceptor graphene-based hybrid materials for managing charge-transfer phenomena, mainly, but not exclusively, with porphyrins and phthalocyanines are presented. Earlier examples and studies performed on graphene oxide modified with organic electron donors are also given.

Keywords: donor-acceptor; electron-transfer; functionalization; graphene; photophysical properties

Introduction

Among the outstanding forms of carbon nanostructures, graphene, a single atom layer of carbon, is a newly available material exhibiting unique mechanical [1] and electronic properties [2] and can be described as one of the most examined materials of recent years [3], [4]. Diverse approaches have been developed to obtain graphene sheets, including mechanical cleavage of graphite [3], chemical vapor deposition on metal surfaces [5], [6], liquid exfoliation via sonication [7], [8], dissolution in superacids such as chlorosulfonic acid [9] and ball milling [10]. However, a major drawback in graphene, likewise carbon nanotubes, stems from its insolubility in all solvents, thereby bringing obstacles for chemical manipulation toward applications. In this frame, two are the main routes to overcome the above hurdle. Namely, through water-soluble graphene oxide (GO), which can be reduced to the so-called reduced-graphene-oxide (RGO), followed by post-modification to acquire functionalized graphene [11]. However, as reduction of GO partially occurs, while sometimes leads to amorphous carbon [12], restoration of the graphene sp^2 network is incomplete and therefore the properties of the resulting RGO significantly deviate from those of pristine graphene. Hence, the particular approach should not be considered suitable when targeting applications in which the novel electronic properties of graphene are of primary importance. Alternatively, wet exfoliation of graphite followed by functionalization is a more efficient strategy. Although functionalization of exfoliated graphene can be achieved by either covalent anchoring of organic addends onto graphene lattice [13] or supramolecularly, by π-π stacking and/or van der Waals means [14], the latter methodology suffers from weak interactions developed between the two species (i.e. graphene and organic units), which often times leading to leakage of the organic part. Apparently, covalent functionalization of exfoliated graphene, in which the organic unit is tightly attached on the graphene network, is the method of choice for preparing novel donor-acceptor hybrid materials potentially suitable for managing photoinduced electron-transfer phenomena.

Single-layer, bilayer and oligo-layer graphene sheets have been utilized to fabricate donor-acceptor ensembles potentially useful in energy conversion schemes. Actually, electrons can travel without scattering around the 2D crystal structure of graphene [15], thus guaranteeing a continuous lossless electron flow. In addition, considering that carbon nanotubes are generally produced as a mixture of metallic and semiconducting components, while also sometimes retain

significant amounts of metal nanoparticles as impurities, it is easily understood the advantageous character of graphene when employed in the construction of donor-acceptor systems. In this frame, although the field is in its infancy, a few hybrid materials composed of graphene and photoactive components, such as for example porphyrins and phthalocyanines, have been prepared and evaluated toward photoinduced charge transfer phenomena [16] [17] [18]. Moreover, semiconducting quantum dots such as CdS [19] [20] [21] [22], CdSe [23] [24] [25] [26], CdTe [27] [28], ZnO [29] [23] and cooperative mixtures of them for instance with Au nanoparticles [31] [32] have been incorporated to graphene sheets (GO or rGO) yielding donor-acceptor systems. However, the scope of the current mini-review is to highlight recent advances in the preparation of graphene-based hybrid materials only with organic electron donors for energy conversion. Prior of that, routes and strategies for the chemical functionalization of graphene with photoactive electron donors will be presented, as well as common techniques for the characterizing and evaluating the photophysical properties of the materials will be discussed.

Results and Discussion

Chemical functionalization toward formation of donor-acceptor hybrids

A plethora of soluble and easy-to-handle graphene-based materials have been prepared and methodologies for the functionalization of graphene have already been reviewed [12, 33, 34, 35, 36, 37]. In Scheme 1 a collection of the major chemical reactions leading to the covalent modification of graphene framework are displayed. Briefly, after the exfoliation of graphite, the following reactions can be performed to modify the graphene sheet (summarized in Scheme 1):

(a) [3+2] 1,3-dipolar cycloaddition of in-situ generated azomethine ylides, resulting on the introduction of fused pyrrolidine rings onto the skeleton of graphene [38]. Azomethine ylides are organic 1,3-dipoles possessing a carbanion next to an immonium ion and can be readily produced upon decarboxylation of the immonium salts derived from the condensation of α-amino acids with aldehydes or ketones. When azomethine ylides are added to graphene, a fused pyrrolidine ring is formed on the junction between two six-membered rings of the graphene lattice. Notably, functionalized aldehydes lead to the formation of 2-substituted pyrrolidines, whereas reaction with N-substituted glycines leads to N-substituted pyrrolidines, thus allowing the preparation of numerous custom-synthesized graphene-based materials;

(b) [1+2] cycloaddition of malonate derivatives, so-called Bingel reaction, yielding cyclopropane rings on graphene [39]. This versatile modification involves the generation of carbon nucleophiles from α-halo esters and their subsequent regioselective addition to graphene. In general, the addition takes place on double bonds between two six-membered rings present on graphene, yielding methano-modified graphene-based materials. Moreover, modifications of the original Bingel reaction exist, utilizing (i) carbanionic precursors to methano-modified graphene other than malonates, and (ii) alternative pathways generating the reactive monohalomalonate intermediate in situ;

(c) addition of in-situ generated aryl diazonium salts, proceeding via the release of dinitrogen [40]. The reaction mechanism involves electron transfer from graphene to the diazonium salt, resulting in the formation of a radical aryl unit, which subsequently adds to the sp^2 carbon lattice of graphene;

(d) addition of azides forming aziridine adducts onto graphene [41]. The particular functionalization proceeds via nitrenes as generated upon the thermal (or photochemical) decomposition of azides and the liberation of dinitrogen.

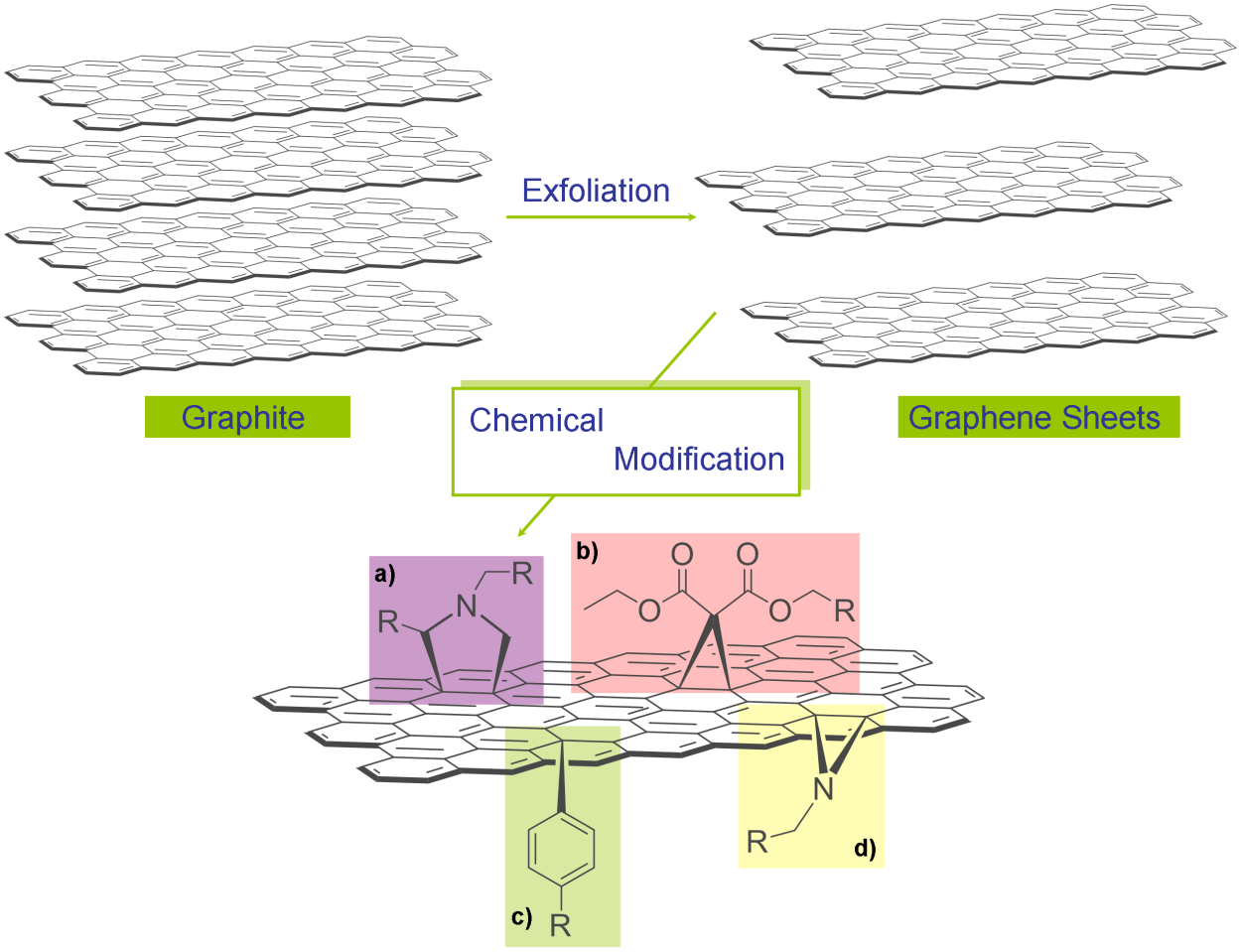

Scheme 1. General chemical modification routes for exfoliated graphene sheets. (a) [3+2] 1,3-dipolar cycloaddition of in-situ generated azomethine ylides, (b) [1+2] Bingel cycloaddition, (c) aryl diazonium addition, and (d) azide addition.

Characterization, charge-separation and incident-photon-to-current efficiency

Raman spectroscopy is an extremely useful tool for characterizing graphene-based materials. Intact graphite exhibits two main characteristic bands, namely the G-band, due to the presence of sp^2 hybridized carbons at 1585 cm^{-1} and the higher-frequency band 2D at around 2725 cm^{-1}. In addition, functionalized graphene sheets show the emergence of a new band, the so-called disorder D-band at around 1350 cm^{-1}, due to the presence of sp^3 hybridized carbons – defects and/or anchored sites where functionalization occurs, while also the 2D band is found changed as it shifts to lower frequency and stiffens when compared to the corresponding one of graphite. Thermal gravimetric analysis gives information about the functionalization degree in modified

graphene because the covalent attachment of the organic moieties can be thermally eliminated, while intact graphite is thermally stable under an inert atmosphere. Moreover, microscopy techniques such as TEM and AFM offer significant insight regarding the morphology of graphene and especially the number of layers that exist in a particular sample. Overall, based on such complementary spectroscopic, microscopy and thermal techniques graphene-based nanohybrids can be qualitatively monitored, while at the same time evidence about the dimensions and purity is obtained.

Within the frame of energy conversion schemes, the challenge for constructing robust and functional architectures made of graphene and photo- and/or electro-active components is met by considering and applying to large extent the aforementioned functionalization strategies. In that respect, a few covalently linked graphene sheets with organic electron donor moieties for managing photoinduced electron-transfer processes have been synthesized. Briefly, photoinduced excitation of the organic electron donor in the graphene-based nanohybrid, results on the formation of the singlet-excited state of the organic component. Then, charge-separation takes place and the efficiency of the whole process is governed by how fast or slow the recombination of charges occurs. A simplistic approach for such a process, which sometimes may be quite complex involving triplet states as derived upon intersystem crossing, is schematically presented on Scheme 2.

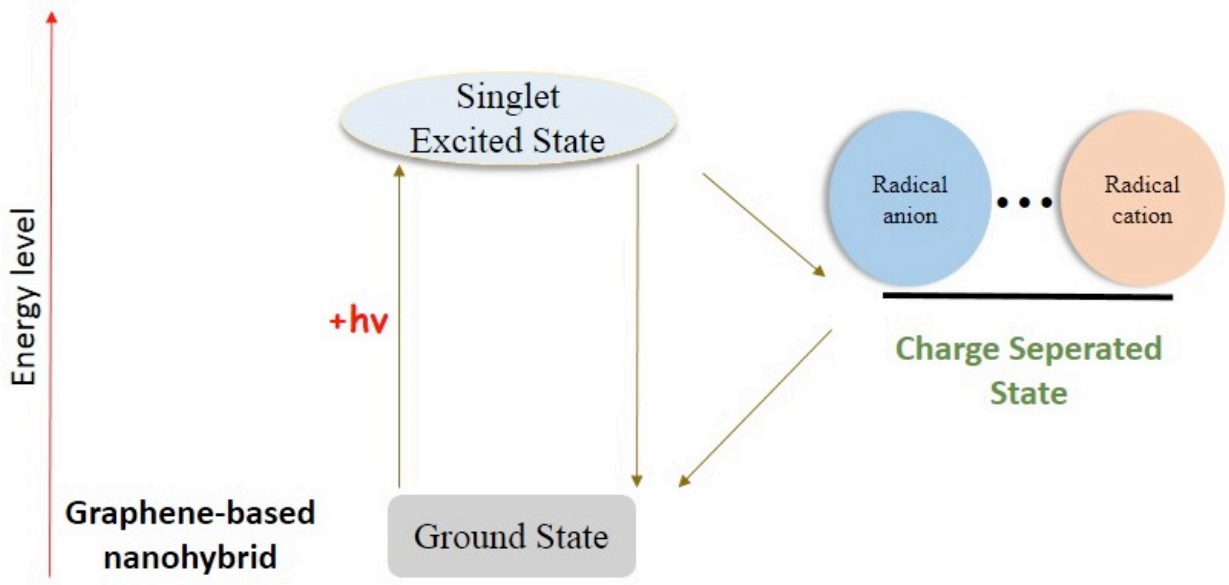

Scheme 2. Illustrative energy diagram for the photoinduced formation of the charge-separated state of graphene-based hybrid materials.

Usually, the photoelectrochemical measurements of graphene-based hybrid materials with photoactive organic electron-donors are carried out in a three-compartment cell using a potentiostat, employing a saturated calomel reference electrode, a working electrode and a Pt wire gauze counter electrode. The latter kind of configuration allows performing photocurrent measurements under electrochemical bias. Electrophoretic deposition is applied to fabricate films of the graphene-based hybrid material onto an optically transparent electrode (OTE) and nanostructured SnO_2 films cast onto the OTE. Typically, the procedure is as below: a suspension of the graphene-based hybrid material (~2 mL) in THF is transferred to a 1 cm cuvette, then, two OTE cut from conducting glass were inserted, and a dc electric field (~100 V/cm) is applied. The graphene-based hybrid material from the suspension is driven to the positive electrode surface, and a robust thin-film (abbreviated as OTE/SnO_2/graphene-based hybrid material) is deposited within a short period of time. The photocurrent action spectrum of the OTE/SnO_2/graphene-based hybrid material electrode was evaluated by examining the wavelength dependence of the incident-photon-to-current-conversion-efficiency (IPCE). The IPCE values are calculated by normalizing the photocurrent densities for incident light energy and intensity and by using the following equation:

$$IPCE(\%) = 100 \times 1240 \times i/(W_{in} \times \lambda)$$

where, i is the photocurrent density (A cm^{-2}), W_{in} is the incident light intensity (W cm^{-2}), and λ is the excitation wavelength (nm).

Donor-acceptor hybrids based on graphene-oxide or reduced graphene oxide

The unique and notable features of porphyrins and phthalocyanines as light-harvesting antennas that capture visible light with high extinction coefficients and remarkable redox properties put them in pole position as suitable electron donors to be associated with graphene. The very first approach on associating porphyrins with graphene was made by condensing an amino-modified tetraphenylporphyrin (TPP) to the carboxylic functionalities present on GO [42] furnishing the GO-TPP hybrid structure shown in Scheme 2. The observed luminescence quenching of TPP in the GO-TPP hybrid material is indicative of strong intrahybrid electronic communication between TPP and GO in the excited state. Possible pathways for the fluorescence quenching of the TPP are attributed either to photoinduced electron or energy transfer to GO. Additionally, the formation of the charge-separate state $(GO)^{\bullet-}$-$(TPP)^{\bullet+}$ was identified possessing

0.87 eV energy gap, while the incident-photon-to-photocurrent-efficiency (IPCE) was calculated as 1.3% [43].

Along the same lines, when hydroxy-functionalized porphyrin (H_2P) was condensed to GO sheets, the GO-H_2P hybrid material showed enhanced non-linear-optical (NLO) properties, which are mainly ascribed to photoinduced electron transfer reactions occurring from H_2P to GO within the nanoensemble [44]. Similarly an amino-modified zinc phthalocyanine (ZnPc) was conjugated to GO furnishing the GO-ZnPc hybrid which showed enhanced NLO properties due to strong interaction between the donor and acceptor components [45].

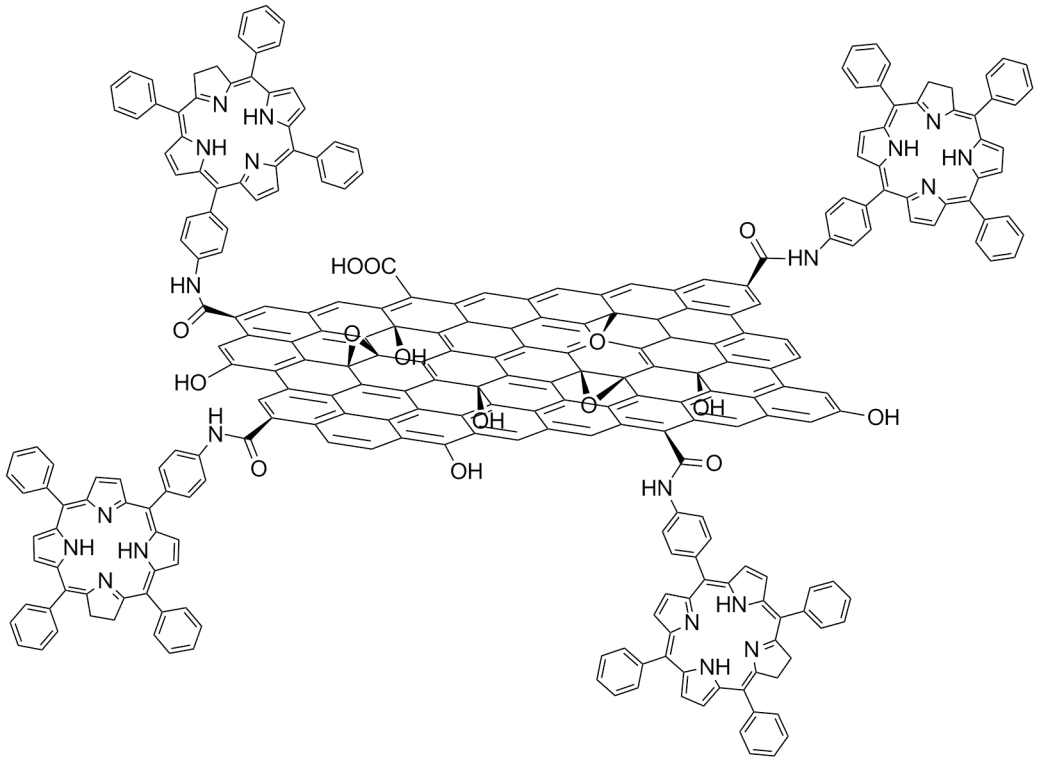

Scheme 2. Tetraphenyl porphyrin (TTP) condensed on graphene oxide (GO) yielding GO-TPP hybrid material. [42]

On a different route to associate porphyrin units with GO, an imidazolium ionic-liquid type addend was initially conjugated to GO forming an amide bond. The presence of the positively charged imidazolium moiety allows modulating the dispersibility of the modified GO material from aqueous media to organic solvents by simply exchanging and altering the counter anion of the imidazolium unit. More importantly, when an anionic porphyrin was incorporated as

counter anion of the GO-based ionic-liquid type hybrid material, electronic interactions between the porphyrin and the GO lattice were identified [46].

Zinc(II) phthalocyanine (ZnPc) as electron donor and C_{60} were added to GO through esterification reaction between carboxyl groups of GO and hydroxyl groups present on ZnPc as well as on a fullerene derivative. Photoexcitation of ZnPc-GO-C_{60} at 390 nm, wavelength at which ZnPc is predominantly excited, resulted on the identification of the first singlet excited state of ZnPc. However, photoexcitation at 532 nm, at which C_{60} is mainly excited, revealed the formation of both the ZnPc radical cation and C_{60} radical anion. The latter results, as obtained from nanosecond transient absorption spectroscopy measurements, ascertain the formation of the charge-separated state in ZnPc-GO-C_{60} hybrid material [47].

Recently, the fabrication of a photoinduced charge-transfer composite between GO and ferrocene moieties (GO-Fc according to Scheme 3) was reported [48]. Although, the study refers to graphene oxide, it is the first report that combines graphene and ferrocene properties via chemical complexation. Photoresponsivity of the developed composite was investigated by fabricating a Au/GO-Fc/Au device. Interestingly, significant enhancement in current density under illumination of light was observed, thus suggesting charge-transfer processes within the GO-Fc hybrid material.

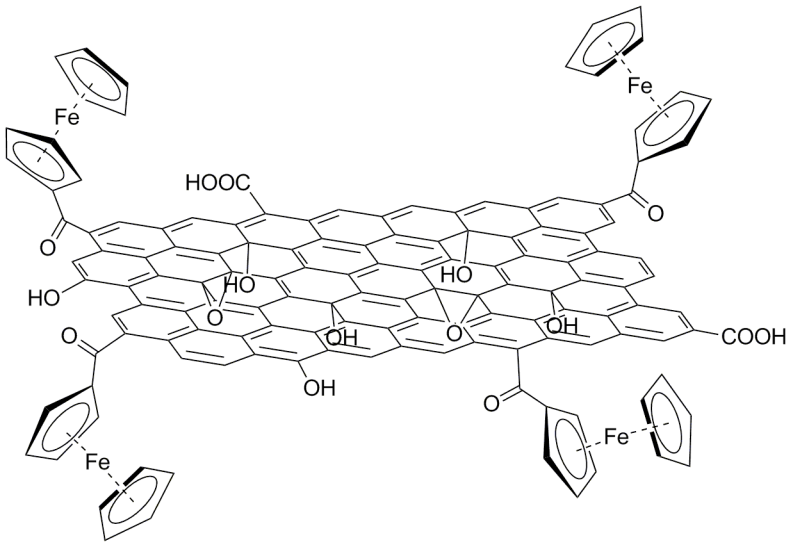

Scheme 3. Ferrocene units anchored on graphene oxide (GO) forming GO-Fc hybrid material, used in photoinduced charge-transfer phenomena. [48]

As described above, cations of transition metals are often present in chromophores (central metal core of Pcs, porphyrins etc.) and take part to the electron/energy transfer processes. On a very recent approach, a terpyridine (tpy) derivative, as ligand for Fe(II) ions, was used to modify graphene oxide [49]. In more detail, Fe(II) coordinates tpy groups of the upper surface of such graphene sheets with the same groups of the lower surface of another graphene layer, promoting self assembly of GO. The Fe-tpy-GO nanohybrid fully decomplexes when treated with EDTA and re-complexes after fresh addition of Fe(II) (Scheme 4). Furthermore, Fe-tpy-GO tested as catalyst for the oxygen reduction reaction (ORR) and found to be durable against carbon monoxide poisoning and with higher fuel selectivity compared with commercially available Pt/C electrocatalysts. As already underlined, the ORR reactivity was tightly connected with electron transfer processes, thus indicating an indirect way to detect these phenomena. Ruthenium(II) also employed as a coordinating cation and resulted to a Ru-tpy-GO hybrid material with enhanced photocurrent response, higher than GO and Fe-tpy-GO, probably due to more effective electron transfer from the Ru-tpy core to the graphene network. This class of self-assembled covalently functionalized GO-based nanohybrids is a promising new member in the family of graphene hybrid materials with potent application in energy conversion and storage.

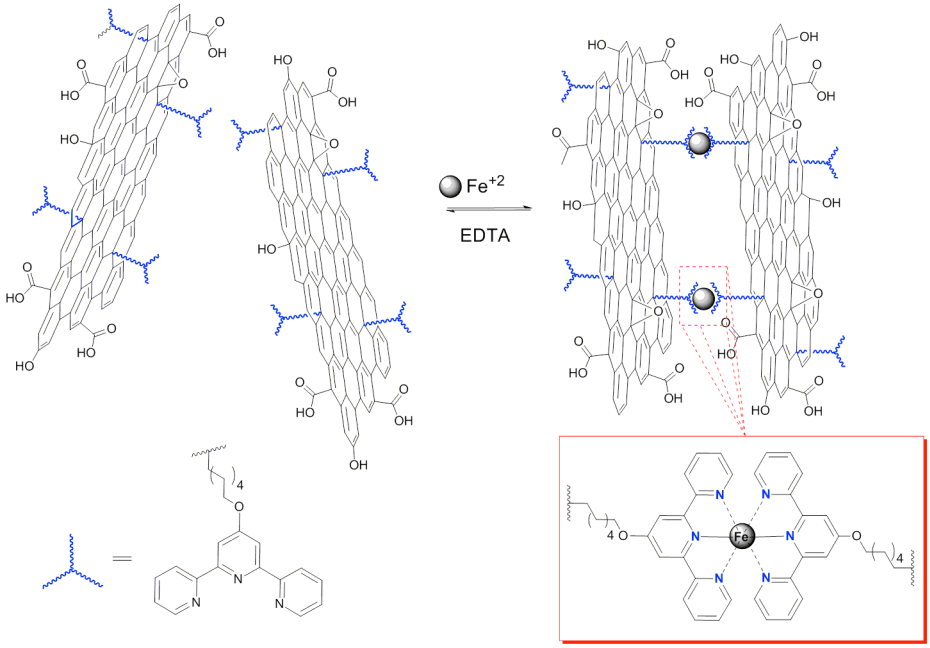

Scheme 4. Iron(II) coordinated on terpyridine (tpy) moieties covalently anchored on graphene oxide (GO) forming GO-tpy-Fe hybrids. [49]

On similar grounds, as far as RGO concerns, the latter was initially modified by phenylacetylene units, which were used to mediate the grafting of zinc-porphyrin (ZnP) and ruthenium-phenanthroline (RuP) chromophores *via* a copper-catalyzed "click" chemistry reaction [50]. As an example, in Scheme 5 is illustrated the preparation of the RuP-RGO hybrid material. The excellent dispersibility of the two novel types of graphene-based nanostructures in common organic solvents allowed their easy characterization by various microscopy and spectroscopic techniques. Spectroscopic results in ground and excited states gave noteworthy insights for intra-hybrid electronic communication between the chromophore moiety and RGO, leading to the fabrication of photoelectrochemical cells. The photo-induced electron transfer properties of the ZnP-RGO and RuP-RGO were evaluated by examining their photocurrent responses in thin films on ITO for the on/off light illumination cycles.

In all the above studies, charge-transfer interactions within donor-acceptor graphene-based ensembles were exploitation in the field of energy conversion. However, the unique properties of graphene and in particular its ability to efficiently quench the photoinduced emission of electron donors have recently been diversely utilized. Thus, it is interesting to note that, although graphene-based biomaterials are out of the scope of this mini-review, GO was covalently functionalized with peptides, antibodies and other biomolecules targeting applications in diagnostics, novel therapeutic approaches and near infrared (NIR) photothermal therapies [51]. A representative work demonstrating the activated fluorescent imaging probe is based on a GO-coumarin conjugate with high sensitivity in cancer cell visualization [52]. In this context, it was developed a graphene-based nano-probe having a fluorescence off–on response for intracellular imaging via covalently linking coumarin derivatives to GO through disulfide bonds. The obtained nano-probe shows no or weak fluorescence (OFF) due to the fluorescence quenching due to energy/electron transfer mechanism from the coumarin moiety to GO. Nevertheless, it becomes activated (ON) inside the cells by glutathione-initiated dissociation, showing remarkably enhanced fluorescence.

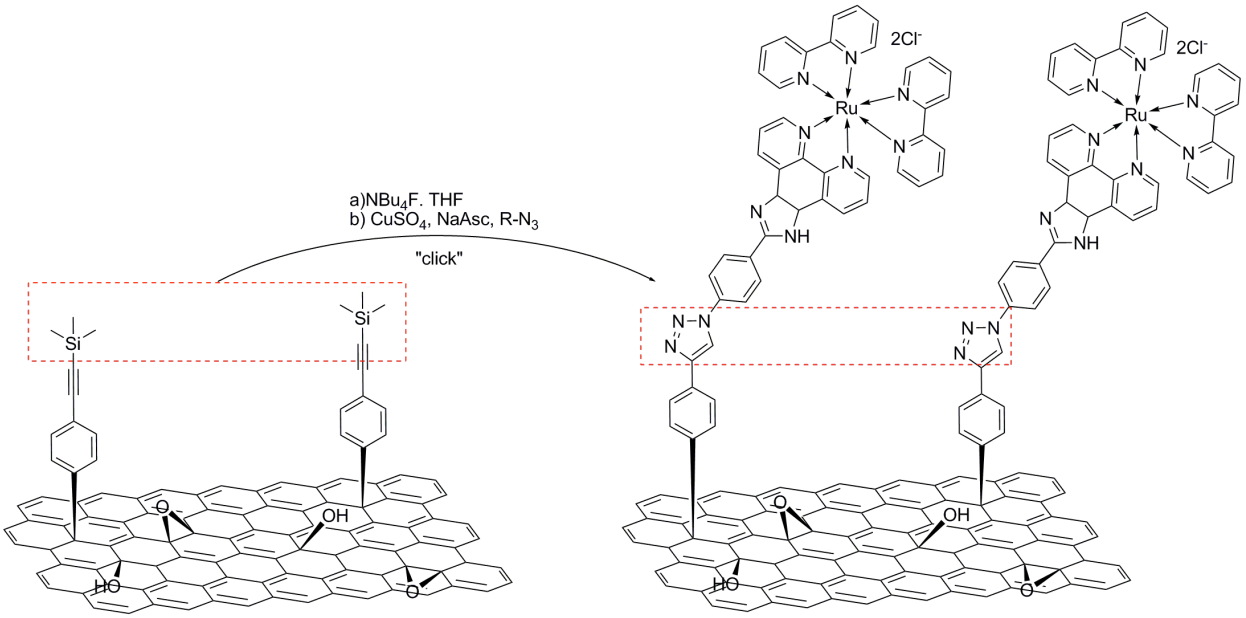

Scheme 5. "Click-reaction" for the grafting of a porphyrin onto reduced graphene oxide (RGO) sheets pre-modified by phenylacetylene units. [50]

Donor-acceptor hybrids based on exfoliated graphene

However, as mentioned earlier, the presence of many surface defects disrupting the sp^2 network in GO, influence the quality of the electronic and optical properties of the hybrid materials. Therefore, moving beyond defected GO, free TPP as well as Pd-metallated TPP were introduced onto graphene as substituents of pyrrolidine rings formed upon the 1,3-dipolar cycloaddition reaction of azomethine ylides on exfoliated graphene [53]. In this approach, graphite flakes were initially sonicated in o-DCB to induce exfoliation. In the following step sarcosine and the corresponding aldehydes bearing the TPP and Pd-TPP moieties were added and the reaction mixture was stirred at 160 ^{o}C under N_2 for one week to yield the structures shown in Scheme 6. The presence of TPP or Pd-TPP in the graphene-based hybrid materials was confirmed by standard spectroscopic methods, such as UV-Vis, Raman, FTIR and XPS. Complementary electron microscopy studies showed that the functionalization processes did not affect the morphology of graphene in the hybrid materials. More importantly, fluorescence and phosphorescence quenching of either the free or Pd-metallated porphyrin was observed, with simultaneous decrease on the fluorescence emission lifetimes. These observations are indicative of intrahybrid interactions in the excited state through energy- and/or electron-transfer between

graphene and the covalently bound porphyrin moieties. Noteworthy, the particular type of functionalization resulted on a relatively low loading of porphyrins on graphene, as calculated by thermogravimetry for the two hybrid materials, thus preserving to large extent the π-electronic network of graphene and render them suitable for solar and/or photoelectrochemical cells applications.

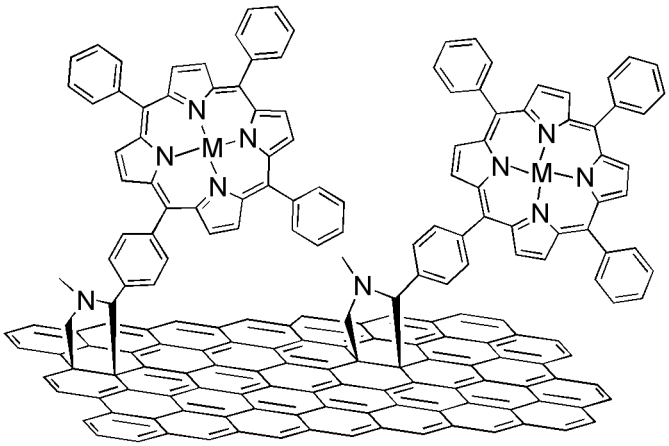

M= H, Pd

Scheme 6. Free and Pd-metallated tetraphenyl porphyrin moieties as substituents of pyrrolidine rings covalently anchored on exfoliated graphene. [53]

Along the same lines, another graphene-based hybrid material was prepared in which a porphyrin was anchored to graphene following a Suzuki coupling reaction between iodophenyl-functionalized graphene and the corresponding porphyrin boronic ester [54]. The covalently linked graphene–porphyrin hybrid was especially designed to possess a short, yet rigid phenylene spacer between the porphyrin and the graphene. Photophysical measurements revealed the presence of a short-lived porphyrin singlet excited state (38 ps), however, without yielding the porphyrin radical cation, thus suggesting that energy transfer from the porphyrin excited state to the graphene sheets occurs. Moving a step forward, a prototype photoelectrochemical device, in which a SnO_2 electrode was coated with the aforementioned graphene-porphyrin hybrid material, was constructed. Photophysical and electrical measurements revealed the absence of any photocurrent response from the porphyrin absorption, leading to a maximum IPCE value of approximately 3%.

Further surveying the functionalization of graphene with organic electron donors, phthalocyanines were introduced on exfoliated graphene in parallel and via two independent

routes. With the first approach, covalent grafting of (2-aminoethoxy)(tri-tert-butyl) zinc phthalocyanine (ZnPc) to exfoliated graphene sheets via direct nucleophilic addition of primary amines was accomplished (Scheme 7) [55]. The ZnPc-graphene hybrid material was extensively characterized by complementary spectroscopic means as well as electron microscopy. Efficient fluorescence quenching of ZnPc in the ZnPc-graphene hybrid material was observed and the deactivation pathway was evaluated by femtosecond transient absorption spectroscopy. The charge-separated state $ZnPc^{\bullet+}$–$graphene^{\bullet-}$ was identified. An electrode of the ZnPc-graphene hybrid material was prepared and its photoelectrochemical properties were examined. It was found to exhibit stable and reproducible photocurrent responses, and the incident photon-to-current conversion efficiency was determined to be 2.2% at 420 nm. The later results highlight the important role of the covalent grafting of ZnPc onto the graphene sheet for enhancing the photoinduced electron-transfer phenomena between the two components and achieving higher IPCE values as compared to non-covalently interacting ZnPc [56], as well as ZnPc-based oligo-phenylenevinylene oligomers [57] with graphene.

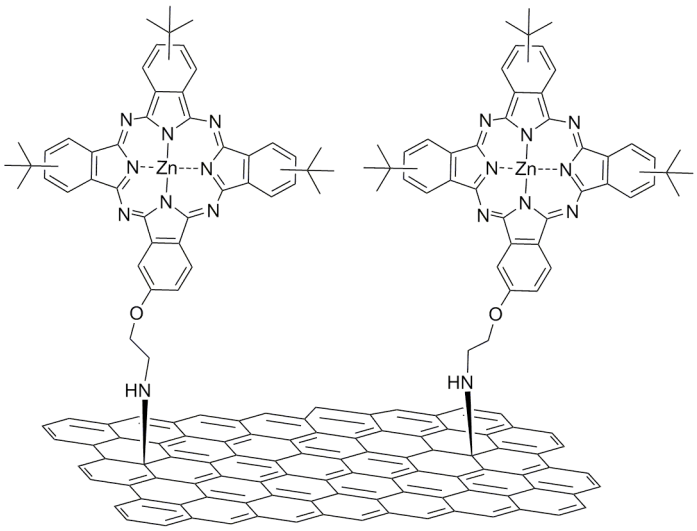

Scheme 7. Covalent grafting of (2-aminoethoxy)(tri-tert-butyl) zinc phthalocyanine to exfoliated graphene sheets via direct nucleophilic addition of primary amines. [55]

In the second strategy followed for the realization of a Pc-graphene hybrid, a few-layered graphene dispersion as obtained by exfoliating graphite upon sonication, was utilized. The exfoliated graphene sheets were then reacted in the presence of excess N-methylglycine and 4-formylbenzoic acid to yield functionalized graphene carrying pyrrolidine rings with pendant

phenylcarboxylic acid units. In the next step, condensation between the –COOH units of the pre-functionalized graphene and mono-OH derivatized phthalocyanine, in the presence of EDC/HOBt as activators, afforded the graphene-Pc hybrid material (Scheme 8) [58]. Photoexcitation of Pc-graphene and evaluation of the species developed by pump-probed femtosecond transient absorption spectroscopy, revealed the formation of the radical anion of graphene, as a broad band in the NIR region. Based on multiwavelength analysis a short-lived and a long-lived component with lifetimes of 3.3 and 270 ps, respectively, in DMF, were identified, suggesting that the ultra fast charge-separation in the Pc-graphene is followed by a slower charge-recombination.

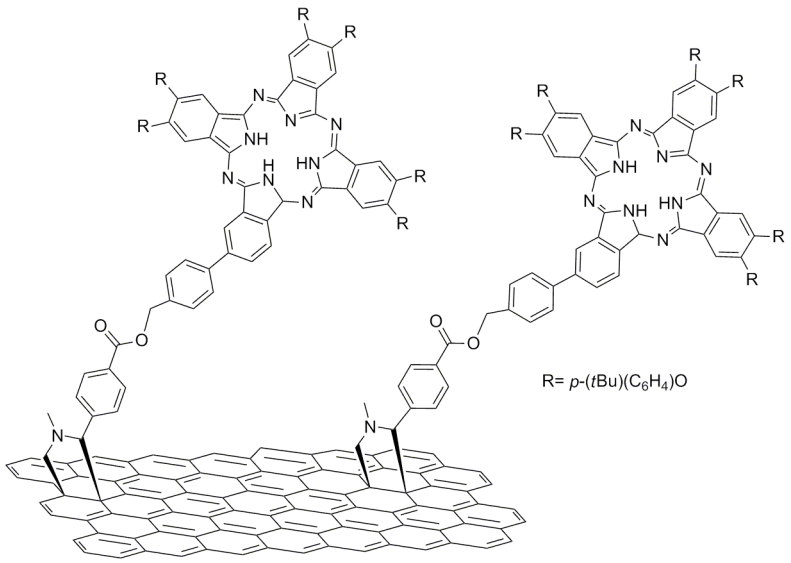

Scheme 8. Phthalocyanine-graphene hybrid material, prepared upon condensation of mono-OH derivatized phthalocyanine with pendant phenylcarboxylic acid units present as substituents of pyrrolidine rings on pre-modified graphene sheets. [58].

Recently, a sulfonyl-substitute zinc phthalocyanine was custom-synthesized and covalently bound via “click” chemistry to exfoliated graphene (Scheme 9). Interestingly, due to the strong electron-withdrawing effect of the sulfonyl units, the particular phthalocyanine component acts as electron acceptor in the graphene-ZnPc hybrid material [59]. Complementary electrochemical measurements and photophysical assays, based on fluorescence emission and transient absorption spectroscopy, verified that electron-transfer phenomena exist from graphene to ZnPc.

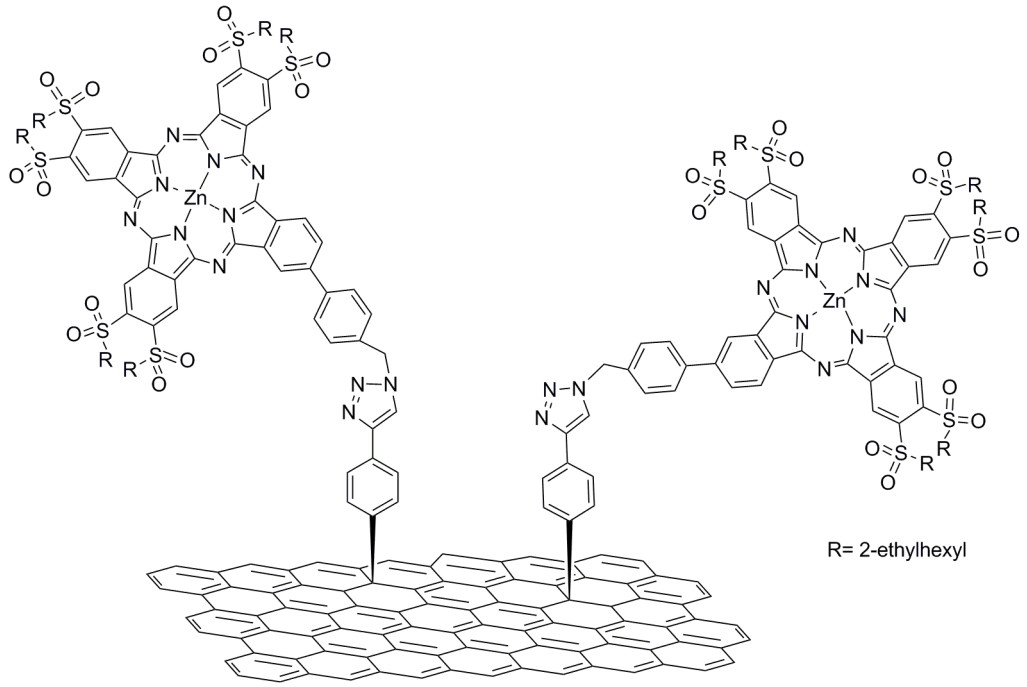

Scheme 9. Sulfonyl-substituted zinc phthalocyanine covalently bound via "click-reaction" conditions to pre-modified graphene. [59]

Beyond the association of porphyrin and phthalocyanine dyes with graphene other photo- and/or electro-active units have been also introduced. In this context, an extended tetrathiafulvalene (exTTF) was grafted to exfoliated graphene with the aid of microwave irradiation upon Bingel reaction (Scheme 10) [39]. The new exTTF-graphene material was fully characterized by spectroscopic, thermal, and microscopy means. Importantly, the electrochemical properties of exTTF-graphene were studied by cyclic voltammetry and allowed to identify the formation of a radical ion pair that includes one-electron oxidation of exTTF and one electron reduction of graphene.

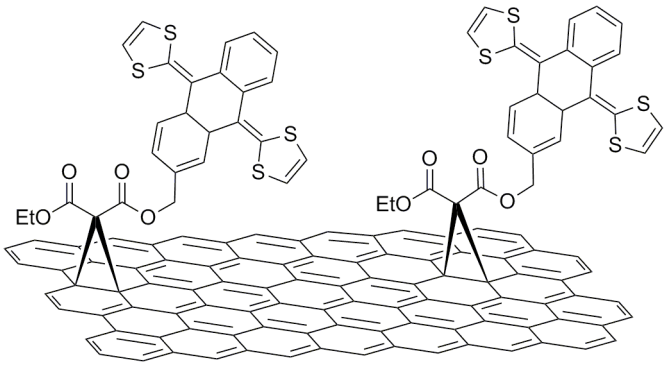

Scheme 10. Extended tetrathiafulvalene units covalently attached to exfoliated graphene via Bingel cycloaddition reaction. [39]

Covalently functionalized few-layer graphene with the bipyridine ruthenium complex (2,2′-bipyridyl)-4-pyridyl-chlororuthenium (II), abbreviated as $Ru(bpy)_2(py)Cl$, results on the formation of another novel nanohybrid material (Scheme 11). In the latter, the slow recombination of the photoexcited charges as identified, demonstrates the high potentiality of the hybrid material for immediate applications in photocatalysis as well as in solar energy conversion schemes [60]. The $Ru(bpy)_2(py)Cl$/graphene hybrid material highlights the importance of the covalent binding and the chemistry chosen for the particular functionalization methodology in the photoinduced electron transfer enhancement. Noteworthy, triazole rings constructed by "click" reaction of an alkyne-functionalized graphene sheet (or chromophore) and an azide-functionalized chromophore (or graphene sheet) also shown to amplify the charge transfer [50].

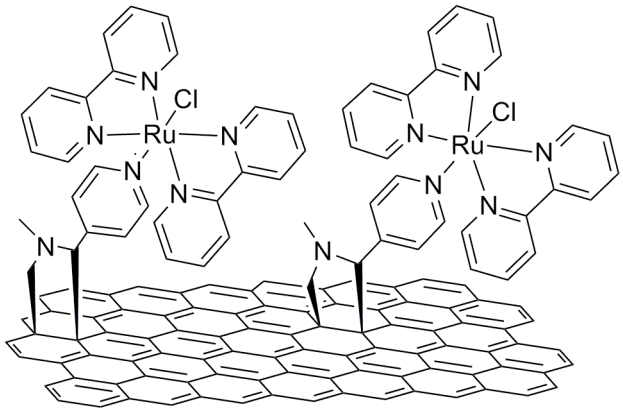

Scheme 11. Covalently functionalized graphene sheets with a Ru-bipyridine complex. [60]

A collection of common photophysical properties for some of the discussed graphene-based nanohybrids is standing in the following Table 1.

Graphene-based hybrid materials [a]	**IPCE** [b]	τ_{CS} **/ ps** [c]	k^{CS} **/ s^{-1}** [d]	Φ^{CS} [e]	τ_{CR} **/ ns** [f]	K^{CR} **/ s^{-1}** [g]	ΔG_{CS} [h]
GO-TPP (S2)	1.3%	675ps(50%) 1600ps(50%)	1.14×10^9	0.77	56ns	1.8×10^7	-1eV

G-TPP(S6)	-	<500ps/6.2ns	-	0.3	-	-	-
G-PdTPP (S6)	-	80ns/660ns	-	<0.01	-	-	-
G-ZnPc (S7)	2.2%	7.7ps		0.98	4.3ns	2.3×10^8	-
G-Pc (S8)	-	3.3ps /270ps	2.03×10^9	0.7	-	-	-
G-sulfonyl PcZn (S9)	-	1ps/600ps	-	-	-	-	-
G-exTTF (S10)	-	-	-	-	-	-	- 0.69eV
G-TPP (ref 31)	3%	30ps	-	-	-	-	-

a. As shown in Schemes 2 and 6-10 and ref. 31

b. The incident-photon-to-current-conversion-efficiency of the fabricated devices.

c. Fluorescence lifetime of the photoexcited hybrids.

d. Fluoresence's quenching rate constant.

e. Quantum yield for charge seperation.

f. Lifetime of the charge seperated state.

g. Charge seperated state's recombination rate constant.

h. Free energy of the charge seperated state.

Conclusions

To summarize, recent advances on the construction of covalent functionalized graphene sheets with photo- and/or electro-active moieties, toward the formation of some novel hybrid materials were overviewed. Although at early stages oxidation was the method of choice for functionalizing graphene, the introduction of numerous lattice defects, that significantly alter the

electronic properties of graphene, required the development of new routes for obtaining graphene sheets that preserve to large extent the high conductivity of the material. Therefore, in recent times, graphene-based hybrid materials are formed by initially exfoliating graphite and followed by chemical functionalization. In this frame, such donor-acceptor graphene-based hybrid materials were synthesized and found to possess interesting optical and photophysical properties. Noteworthy, charge-transfer phenomena mainly occurring from the photoexcited organic chromophore units anchored to graphene layers were realized. Although the potentiality of these materials in applications such as solar and photoelectrochemical cells is great, surely the preparation and properties evaluation of more graphene-based materials is needed in order to further develop and fully document the electronic communication and charge transport processes of the system.

Acknowledgments

Partial financial support from GSRT/NSRF 2007-2013 through action "ARISTEIA II" project FUNGRAPH (3150) "Functionalization of graphene with multichromophoric arrays of photoactive units for energy conversion" is acknowledged.

References

1. Lee, C.; Wei, X.; Kysar, J. W.; Hone J. *Science* **2008**, *321*, 385–388
2. Du, X.; Skachko, I.; Barker, A.; Andrei, E. Y. *Nature Nanotechnol.* **2008**, *3*, 491–495
3. Novoselov, K. S.; Geim, A. K.; Morozov, S. V. Jiang, D.; Zhang, Y.; Dubonos, S. V.; Grigorieva, I. V.; Firsov, A. A. *Science* **2004**, *306*, 666–669
4. Geim, A.K.; Novoselov, K.S. *Nature Mater.* **2007**, *6*, 183–193
5. Li, X.; Cai, W.; An, J.; Kim, S.; Nah, J.; Yang, D.; Piner, R.; Velamakanni, A.; Jung, I.; Tutuc, E.; Banerjee, S. K.; Colombo L.; Ruoff, R. S. *Science* **2009**, *324*, 1312–1314
6. Kim, K. S.; Zhao, Y.; Jang, H.; Lee, S. Y.; Kim, J. M.; Kim, K. S.; Ahn, J.-H.; Kim, P.; Choi, J.-Y.; Hong, B. H. *Nature* **2009**, *457*, 706–710
7. Coleman, J. N. *Acc. Chem. Res.* **2013**, *46*, 14 –22

8. Skaltsas, T.; Karousis, N., Yan, H.J.; Wang, C.R.; Pispas, S.; Tagmatarchis, N. *J. Mater. Chem.* **2012**, *22*, 21507–21512

9. Behabtu, N., Lomeda, J. R., Green, M. J., Higginbotham, A. L., Sinitskii, A., Kosynkin, D. V., Tsentalovich, D., Parra-Vasquez, A. N. G., Schmidt, J., Kesselman, E., Cohen, Y., Talmon, Y., Tour, J. M., Pasquali, M. *Nature Nanotechnology*, **2010**, *5*, 406–411

10. Jeon, I.-Y., Shin, Y.-R., Sohn, G.-J., Choi, H.-J., Bae, S.-Y., Mahmood, J., Jung, S.-M., Seo, J.-M., Kim, M.-J., Chang, D. W., Dai, L., Baek, J.-B. *Proc. Nat. Acad. Sci. USA*, **2012**, *109*, 5588–5593

11. Dreyer, D. R.; Park, S.; Bielawski; C. W. Ruoff, R. S. *Chem.Soc. Rev.* **2010**, *39*, 228–240

12. Gao, W.; Alemany, L. B.; Ci, L.; Ajayan, P. M. *Nature Chem*. **2009**, *1*, 403–409

13. Economopoulos, S. P.; Tagmatarchis, N. *Chem. Eur. J.* **2013**, *19*, 12930–12936

14. Georgakilas, V.; Otyepka, M.; Bourlinos, A. B.; Chandra, V.; Kim, N.; Kemp, K. C.; Hobza, P.; Zboril, R. Kim, K. S. *Chem. Rev.* **2012**, *112*, 6156–6214

15. Geim, A, Novoselov, K. *Nature*, **2007**, *6*, 183-191

16. Bottari, G., Trukhina, O., Ince, M., Torres, T. *Coord. Chem. Rev.*, **2012**, *256*, 2453-2477

17. Chen, Da, Zhang, H., Liu, Y., Li, J. *Energy Environ. Sci.* **2013**, *6*, 1362-1387

18. Dirian, K., Herranz, M.-A., Katsukis, G., Maliq, J., Perez-Rodriquez, L., Romero-Nieto, C., Strauss, V., Martin, N., Guldi, D *Chem. Sci.*, **2013**, *4*, 4335-4353

19. Cao, A., Liu, Z., Chu, S., Wu, M., Ye, Z., Cai, Z., Chang, Y., Wang, S., Gong, Q., Liu, Y. *Adv. Mater.* **2010**, *22*, 103-106

20. Chang, H., Lv, X., Zhang, H., Li, J. *Electrochemistry Comm.* **2010**, *48*, 483-487

21. Pham, T., Choi, B., Jeong, Y. *Nanotechnology* **2010**, *21*, 465603 (10pp)

22. Feng, M., Sun, R., Zhan, H., Chen, Y. *Nanotechnology* **2010**, *21*, 075601 (10pp)

23. Lin, Y., Zhang, K., Chen, W., Liu, Y., Geng, Z., Zeng, J., Pan, N., Yahn, L., Wang, X., Hou, J.-G. *ACS Nano* **2010**, *4*, 3033-3038

24. Wang, T., Zhang, S., Mao, C., Song, J., Niu, H., Jin, B., Tian, Y. *Biosensors and Bioelectronics* **2012**, *31*, 369-375

25. Lightgap, I., Kamat, P. *J. Am. Chem. Soc.* **2012**, *134*, 7109-7116

26. Chen, J., Xu, F., Wu, J., Quasim, K., Zhou, Y., Lei, W., Sun, L.-T., Zhang, Y. *Nanoscale* **2012**, *4*, 441-443

27. Wang, Y., Lu, J., Tang, L., Chang, H., Li, J. *Anal. Chem.* **2009**, *89*, 9710-9715

28. Lu, Z., Guo, C., Yang, H., Quiao, Y., Guo, J., Li, C. *J. Col. Int. Sci.* **2011**, *353*, 588-592

29. Huang, Q., Zeng, D., Li, H., Xie, C. *Nanoscale* **2012**, *4*, 5651-5658

30. Son, D., Kwon, B., Park, D., Seo, W.-S., Yi, Y., Angadi, B., Lee, C.-L., Choi, W.-K. *Nature Nanotechnology* **2012**, DOI: 10.1038/NNANO.2012.71

31. Narayanan, R., Deepa, M., Srivastava, K. *Phys. Chem. Chem. Phys.* **2012**, *14*, 767-778

32. Gu, Z., Yang, S., Li, Z., Sun, X., Wang, G., Fang, Y., Liu, J. *Electrochimica Acta* **2011**, *56*, 9162-9167

33. Chua, C. K.; Pumera, M. *Chem. Soc. Rev.* **2013**, *42*, 3222–3233

34. Rodriguez-Perez, L.; Herranz, M. A.; Martin, N. *Chem. Commun.* **2013**, *49*, 3721–3735

35. Park, J.; Yan, M. Acc. *Chem. Res.* **2013**, 46, 181–189

36. Karousis, N.; Economopoulos, S.; Tagmatarchis N. in *Handbook of Carbon Nano Materials: Materials and Fundamental Applications*, Vol. 4 (Eds.: F. D'Souza, K. M. Kadish), World Scientific, Singapore, pp. 1–54

37. Hirsch, A.; Englert, J. M.; Hauke, F. *Acc. Chem. Res.* **2013**, *46*, 87–96

38. Quintana, M.; Spyrou, K.; Grzelczak, M.; Browne, W. R.; Rudolf, P.; Prato, M. *ACS Nano* **2010**, *4*, 3527–3533

39. Economopoulos, S. P.; Rotas, G.; Miyata, Y.; Shinohara, H.; Tagmatarchis, N. *ACS Nano* **2010**, *4*, 7499–7507

40. Bekyarova, E.; Itkis, M. E.; Ramesh, P.; Berger, C.; Sprinkle, M.; de Heer, W. A.; Haddon, R. C. *J. Am. Chem. Soc.* **2009**, *131*, 1336–1337

41. Liu, L.-H.; Yan, M. *J. Mater. Chem.* **2011**, *21*, 3273–3276; b) Castelain, M.; Martinez, G.; Merino, P.; Martin-Gago, J.; Segura, J. L.; Ellis, G.; Salavagione, H. J. *Chem. Eur. J.* **2012**, *18*, 4965 – 4973; c) Strom, T. A.; Dillon, E. P.;. Hamilton, C. E; Barron, A. R. *Chem.Commun.* **2010**, *46*, 4097–4099

42. Xu Y., Liu Z., Zhang X., Wang Y., Tian J., Huang Y., Ma Y., Zhang X., Chen Y., *Adv. Mater.* **2009***, 21,* 1275–1279

43. Karousis N., Sandanayaka A. S. D., Hasobe, T., Economopoulos S. P., Sarantopoulou E., Tagmatarchis N., *J. Mater. Chem.* **2011**, *21*, 109–117

44. Liu Z.-B., Xu Y.-F., Zhang X.-Y., Zhang X.-L., Chen Y.-S., Tian, J.-G., *J. Phys. Chem. B* **2009**, *113*, 9681–9686

45. Zhao, X., Yan, X.-Q., Ma, Q., Yao, Y., Zhang, X.-L., Liu, X.-L., Tian, J.-G. *Chem. Phys. Lett.* **2013**, *577*, 62-67

46. Karousis, N.; Economopoulos, S. P.; Sarantopoulou, E.; Tagmatarchis, N. *Carbon* **2010**, *48*, 854–860

47. Das S. K., KC C.B., Ohkubo K., Yamada Y., Fukuzumi S., D' Souza F., *Chem. Commun.* **2013**, *49,* 2013–2015

48. Kalita G., Sharma S., Wakita K., Umeno M., Hayashi Y., Tanemura, M., *Phys. Chem. Chem. Phys.* **2013***, 15,* 1271–1274

49. Song S., Xue Y., Feng L., Elbatal H., Wang P., Moorefield C. N., Newkome G. R., Dai L., *Ang. Chem. Int. Ed.* **2014**, *53*, 1415–1419

50. Wang H.-X., Zhou K.-G., Xie Y.-L., Zeng J., Chai N.-N., Li J., Zhang H.-L., *Chem. Commun.* **2011**, *47*, 5747–5749

51. Feng L., Wu L., Qu X., *Adv. Mater.* **2013**, *25*, 168–186

52. Zhang, H.; Huang, R.; Cang, H.; Caib, Z.; Sun, B. *J. Mater. Chem. B* **2014**, *2*, 1742–1750

53. Zhang X., Hou L., Cnossen A., Coleman C. A., Ivashenko O., Rudolf P., van Wess J. B., Browne R. W., Feringa L. B., *Chem. Eur. J.* **2011**, *17*, 8957–8964

54. Umeyama T., Mihara J., Tezuka, Matano Y., Stranius K., Chukharev V., Tkachenko V. N., Lemmetyinen H., Noda K., Matsushige K., Shishido T., Liu Z., Hirose-Takai K., Suenaga K., Imahori H., *Chem. Eur. J.* **2012**, *18*, 4250–4257

55. Karousis N., Ortiz, J., Ohkudo K., Hasobe T., Fukuzumi S., Sastre-Santos A., Tagmatarchis N. *J. Phys. Chem. C* **2012**, *116*, 20564–20573

56. Malig, J.; Jux, N.; Kiessling, D.; Cid, J.-J.; Vázquez, P.; Torres, T.; Guldi *Angew. Chem. Int. Ed.* **2011**, *50*, 3561–3565

57. Brinkhaus, L., Katsukis, G., Malig, J., Costa, R., Garcia-Iglesias, M., Vasquez, P., Torres, T., Guldi, D. *Small*, **2013**, *9*, 2348-2357

58. Ragoussi, M.E.; Malig, J.; Katsukis, G.; Butz, B.; Spiecker, E.; de la Torre, G.; Torres, T.; Guldi, D. M. *Angew. Chem. Int. Ed.* **2012**, *51*, 6421–6425

59. Ragoussi M.E., Katsukis G., Roth A., Malig J., de la Torre G., Guldi D. M., Torres T. *J. Am. Chem. Soc.* **2014**, *136*, 4593–4598

60. Xiao, B., Wang, X., Huang, H., Zhu, M., Yang, P., Wang, Y., Du, Y. *J. Phys. Chem. C.*, **2013**, *117*, 21303-21311

ToC